SAE Aero Design West

Team University of Tulsa Regular
#027

Members:

Jarrod Braun
Kelly Shelts
Ryan Ogilvie
Glenn Lane
Gann Swan
Olivia McGraw
Brian Haiduk
Sanyam Sethi
Al-Yaqadhan Al-Shukaili
Liandong Wang

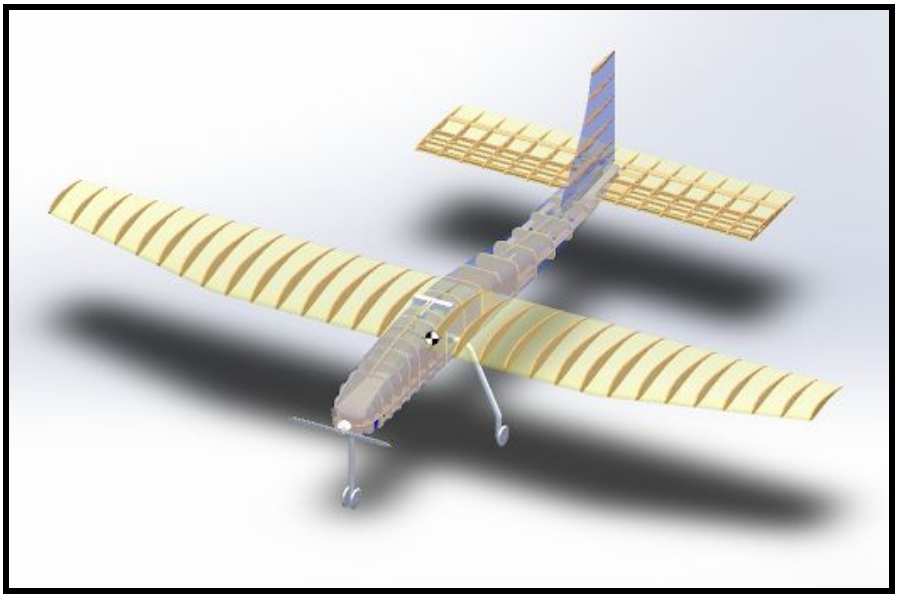

Faculty Advisor:

Dr. Steven Tipton

University of Tulsa

January 26, 2017

APPENDIX A

SAE AERO DESIGN

STATEMENT OF COMPLIANCE

Certification of Qualification

Team Name	University of Tulsa Regular
Team Number	# 027
School	University of Tulsa
Faculty Advisor	Dr. Steven Tipton
Faculty Advisor's Email	smt@utulsa.edu

Statement of Compliance

As Faculty Advisor, I certify that the registered team members are enrolled in collegiate courses. This team has designed, constructed and/or modified the radio controlled aircraft they will use for the SAE Aero Design 2017 competition, without direct assistance from professional engineers, R/C model experts or pilots, or related professionals.

Signature of Faculty Advisor

Team Captain Information:

Team Captain:	Olivia Mcgraw
Captain's E-mail:	Olivia-mcgraw@utulsa.edu
Captain's Phone:	918-946-4441

Note:
A copy of this statement needs to be included in your Design Report as page 2 (Reference Section 4.3)

Table of Contents

List of Figures and Tables:

Executive Summary

The SAE Aero Design Challenge is an annual competition in which graduate and undergraduate students from around the world compete to design, manufacture, assemble, test, and fly the best remote controlled airplane. There are three different classes of the competition: regular, advanced, and micro. TU's Aero Design Team will be competing in the regular class, where the objective is to design an airplane to fly with the maximum number of tennis ball passengers while following the design specifications provided by SAE. The combined aircraft, passenger, and luggage weight must not exceed 55 lbs, and the electric motor must not draw more than 1000 Watts. For the design, the teams must maximize lift, minimize drag, and optimize stability. In manufacturing, the plane must be built as light as possible but be strong enough to withstand the forces of flight and the impact of landing.

The University of Tulsa does not have an aerospace engineering program, so this year's team consists solely of mechanical engineers. The University of Tulsa has competed in five SAE Aero Design Challenges in the past. With the removal of dimensional constraints for this year's competition the team was able to design around a much larger wing to be able to carry more passengers. In past competitions the dimensional rules were what limited the performance of the airplane. However, without these constraints the performance is limited by the wattage constraint and the physical ability to manufacture large wings within the team's facilities.

This year's model enhances TU's last design in aspects of weight reduction, manufacturing, and takeoff distance calculation techniques. The 2017 airplane's decrease in weight comes from a redesigned fuselage. The fuselage is constructed from a combination of pine and balsa wood and only uses aluminum for mounting points for the wing and landing gear. The reduction in dependence on aluminum in the fuselage compared to previous TU planes results in an overall lighter aircraft. Using data obtained from software including XFLR5, SOLIDWORKS, and ANSYS, the team calculated that the 2017 aircraft will be able maintain flight and take off within 200 ft while carrying 15 lbs of payload weight in the form of 24 passengers and their luggage.

Schedule Summary

The 2017 University of Tulsa SAE Aero team was organized in September 2016, although preliminary designs and simulations were done as a research project over the summer of 2016. After the assembly of the team, September and October were spent deciding on a design—a monoplane. After additional research and computer design analysis, the team opted to change to a simpler design in November and decided to focus on making improvements to the 2016 mono-wing plane. November and December were spent designing the new fuselage and figuring out its assembly, redesigning the skeleton of the wings and stabilizers, as well as finalizing calculations and running simulations. January was spent on computer aided design of the final plane design. All materials are being ordered and bought as soon as possible. Plane construction will take place in February, and the team plans to have a first successful flight before February 29. March will used for additional flight testing and final adjustments.

Fuselage Design

An overview and pictures of the complete assembly are shown below. The wing, tail section, and landing strut are shown in Figure 1 for reference. For this fuselage design the tennis balls will be located on the underbelly of the plane and will be loaded from the front. The luggage will be located at the top nose and will be loaded from the front.

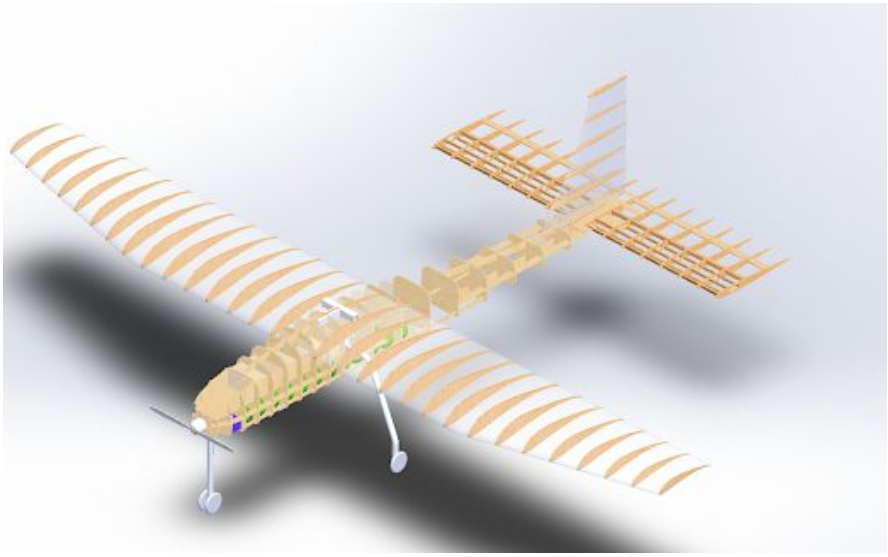

Figure 1: Complete Plane Overview.

The tennis balls will be loaded in from the bottom and a hatch door will keep them in place. The luggage will be loaded in the front and will be housed above the tennis ball in the nose of the plane. Ribs are spaced at the length of a tennis ball (2.7in) to space out the seats for the passengers. The fuselage structure will be primarily made out of pine in order to support the weight of the plane, the passengers, and the luggage. The ribs near the tail, after the last passenger will be made out of balsa wood to save weight. Additionally, an aluminum bar will create a "T" like configuration with the landing gear and goes front the front of the plane to the back landing gear. This is to strengthen the section of the plane which will take the most load including shock loading during landing. The luggage sits directly on top of this bar.

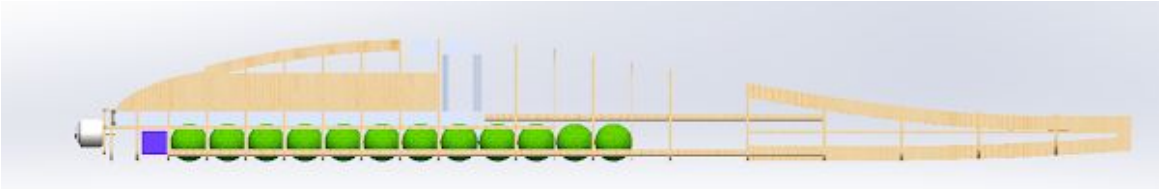

Figure 2: Side View of Loaded Fuselage.

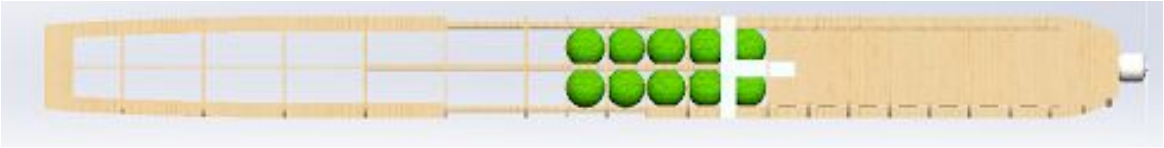

Figure 3: Top View of Loaded Fuselage.

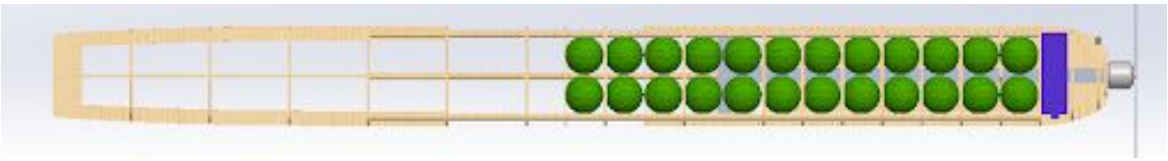

Figure 4: Bottom View of Loaded Fuselage.

The Fuselage will house an estimated 24 passengers. And will carry 12 lbs of luggage. The fuselage empty weight with motor and battery will be an estimated 5lbs

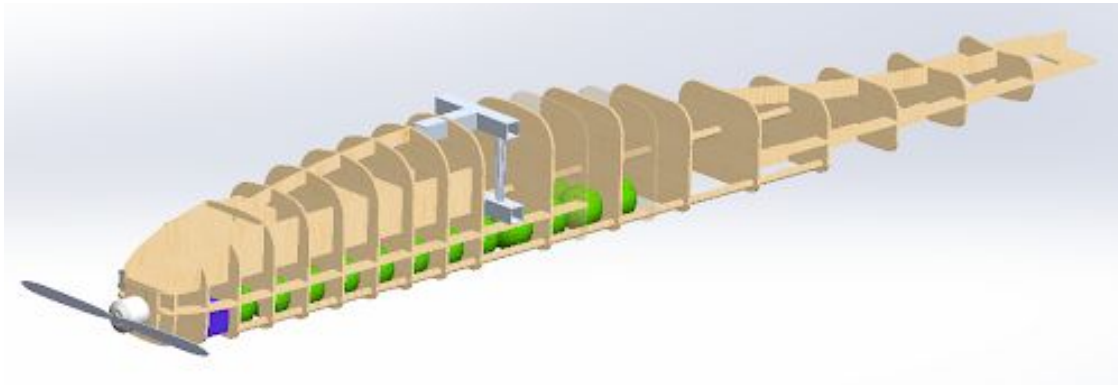

Figure 5: Dimetric View of Loaded Fuselage.

Landing Gear Design

The landing gear will be made from aluminum tubing and will be in tricycle gear configuration. This configuration was chosen as opposed to a taildragger because of risks associated with taildragger aircrafts during take off. A common issue with taildragger configuration at high velocities on the ground is "ground-looping," a rapid and uncontrolled rotation in the yaw direction which can force one wing to touch the ground and incur structural damage. Tricycle gear is more stable for this reason, as long as CG calculations are correct to prevent tipping back while on the ground.

For our design, the nose gear will extend down from a vertical flat surface on the nose of the plane directly behind the propeller. The main gear will be one continuous tube that runs through the fuselage and curves downward on either side. Three total wheels will be at the ends of the tube extending down from the nose and at the two tube ends curving down out of the fuselage.

Wing Design

The first step in the wing design process was to determine which airfoil to use. The team analyzed five high lift airfoils: the NACA 9312, FX74 CL5, CH10, S1210, and S1223. The foils were analyzed using XFLR5 using a base chord length of 1 ft. The analysis was run at a constant Reynold's number of 295,276 and varying angle of attack. The following chart summarizes the findings of the comparisons.

Airfoil	C_L at 0°	C_D at 0°	C_L/C_D at 0°	Max C_L
NACA 9312	0.844	0.019	44.6	1.5
FX74 CL5	1.09	0.025	41.8	1.62
CH10	0.93	0.024	39.5	1.62
S1210	0.99	0.018	55.7	1.77
S1223	1.11	0.02	55.3	1.84

Table 1: Airfoil Analysis.

Based on this data, the team chose the Selig 1223 airfoil for the main wings because it has the highest C_L at zero degrees and the highest maximum C_L. This foil also had a very high ratio of C_L/C_D and a low C_D at zero degrees.

There were four main geometrical criteria the team investigated in designing the wing: span length, root chord length, tip chord length, and taper start location. The taper initiated a backward sweep from the taper start location to the wingtip. The wing maintained the root chord length until the taper start location, and the trailing edge of the wing resided on a single line in all cases. The in-flight and takeoff weight capacities of the tested wings were plotted as each of the geometrical parameters varied. The limiting weight, as referred to in the remainder of this document, is defined as the lower of the takeoff weight and in-flight weights. The process used to determine these weights is detailed in the "Performance Analysis" section of this document.

The first parameter investigated was the span of the wing. The root chord length was held at 18 inches, the tip chord length at 10 inches, and the taper start location at 0 inches from the center of the wing. Figure 6 clearly shows that weight capacity increases with wingspan for both in-flight and takeoff weight. Physical space and manufacturing constraints limited the maximum plausible wingspan to 120 inches, which was chosen for the final design.

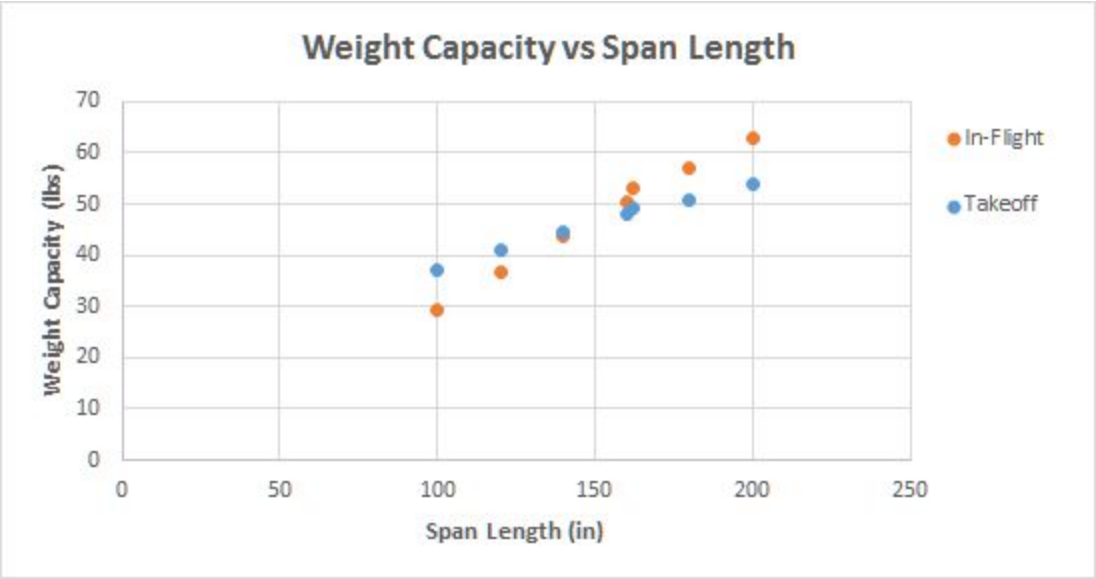

Figure 6: Weight Capacities as Wingspan Varies.

Next the team examined the effect of varying the root chord length between 14 and 22 inches as shown in Figure 7. The wingspan was held at 120 inches, the tip chord length at 10 inches, and the taper start location at 0 inches from the center of the wing. A root chord length of 18 inches was found to produce the highest limiting weight and was selected for the final dimension.

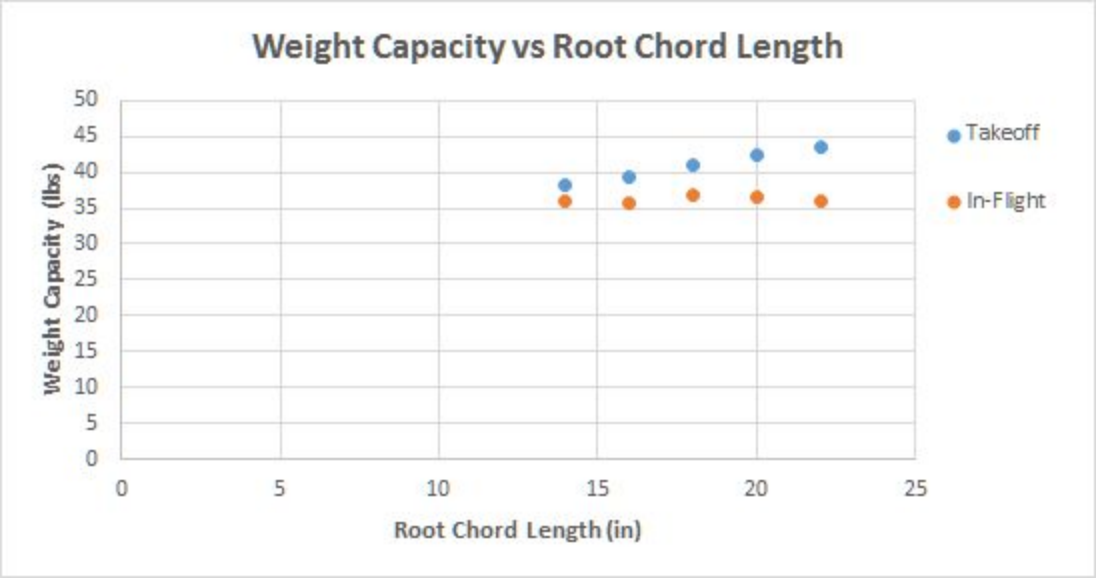

Figure 7: Weight Capacities as Root Chord Length Varies.

The tip chord length was then varied from 6 to 14 inches while the wingspan was held at 120 inches, the root chord length at 18 inches, and the taper start location at 0 inches from the center of the wing. A tip chord length of 10 inches produced the maximum limiting weight, as shown in Figure 8..

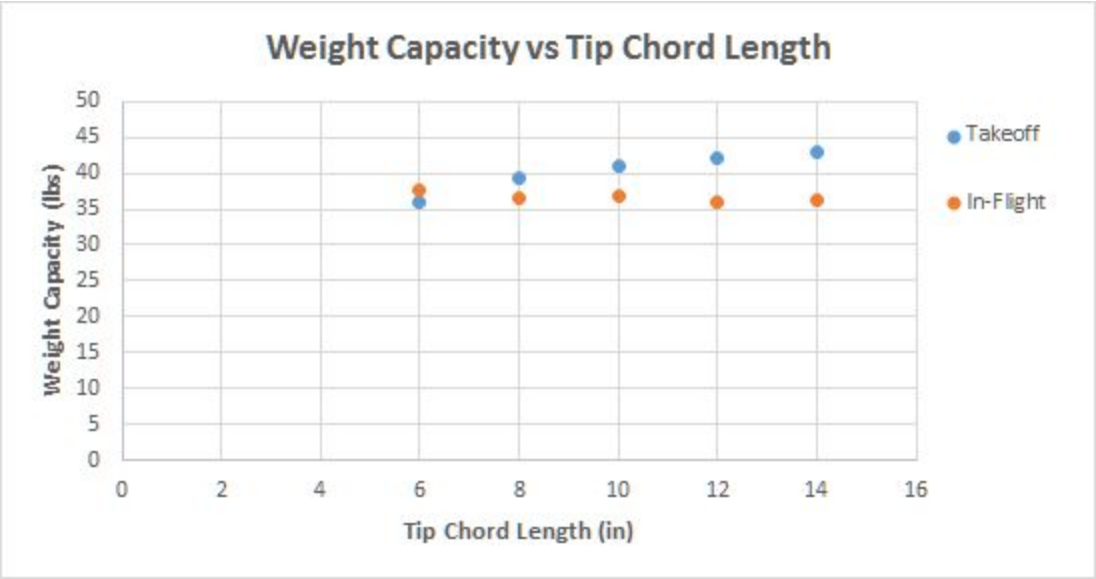

Figure 8: Weight Capacities as Tip Chord Length Varies.

Finally, the team examined the consequences of taper start location, which varied from 0 to 60 inches from the center of the wing as shown in Figure 9. The wingspan was fixed at 120 inches, the root chord length at 18 inches, and the tip chord length at 10 inches. Though the maximum limiting weight occurred at a taper start location of 20 inches, it is easier to manufacture a wing with a taper start location farther from the center. Given that the percent difference for limiting weight between a start location of 20 inches and 30 inches is less than 0.25% the team chose a taper start of location of 30 inches for the final design.

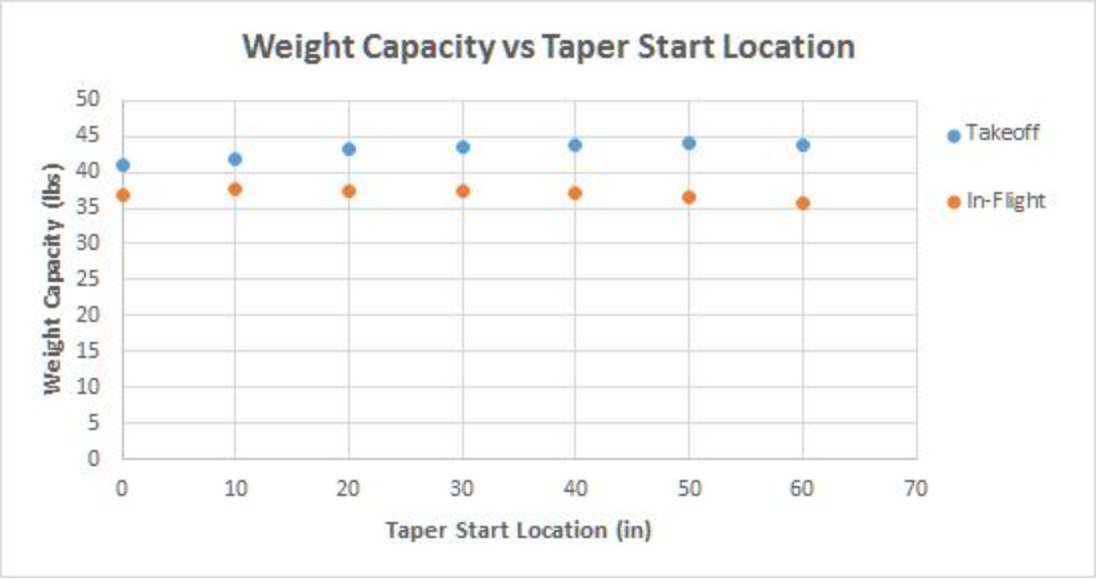

Figure 9: Weight Capacities as Taper Start Location Varies.

The geometric specifications of the wing are summarized in the following table:

Wing Span	120in
Root Chord Length	18 in
Tip Chord Length	10 in
Taper Start Location	30 in
Wing Area	13.336 ft^2

Table 2: Wing Specifications.

Figure 10 below depicts the skeletal final wing design:

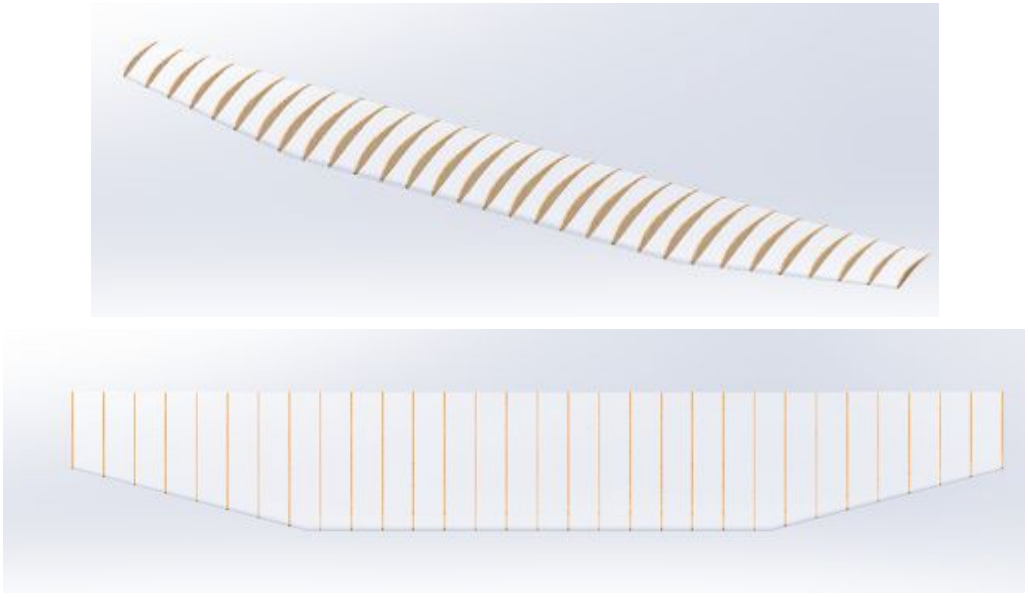

Figure 10: Final Wing Design.

The following table details the lift and drag characteristics of the wing at 0° and 16.5°.

Angle of Attack	**C_L**	**C_D**	**C_L/C_D**
0°	0.760	0.050	15.26
Maximum (16.5°)	2.161	0.239	9.051

Table 3: Wing Performance

Longitudinal Stability

Longitudinal stability is dependent on the horizontal stabilizer, shown below in Figure 11.

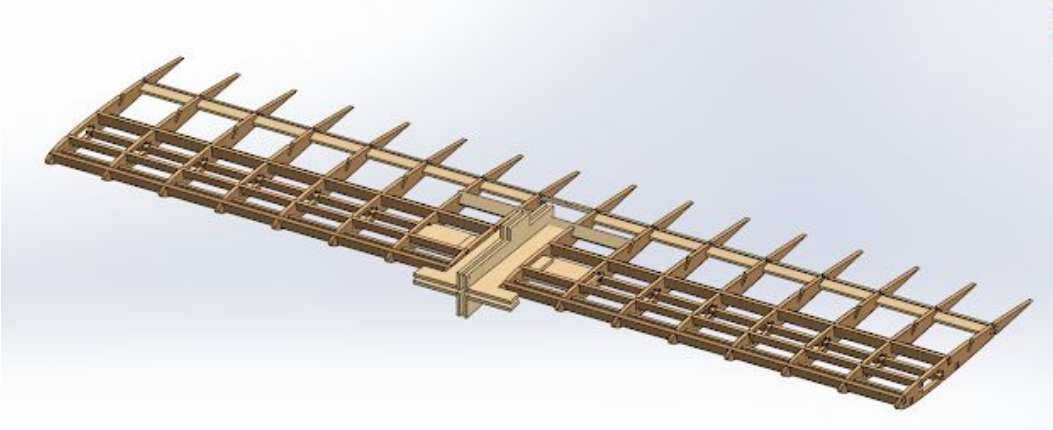

Figure 11: Horizontal Stabilizer (balsa wood).

The effectiveness of the stabilizer is represented in the root locus graph in Figure 12. Each point on the graph represents a longitudinal mode of oscillation. Points to the left of the imaginary axis reflect damped oscillations and points to the right reflect underdamped oscillations. All of the points on the longitudinal root locus graph for this plane are on the left of the imaginary axis, indicating damped oscillations and a stable flight. The real axis corresponds to a frequency of zero, and points further away from this axis have higher oscillatory frequencies. The overall behavior of the plane is a combination of the four modes.

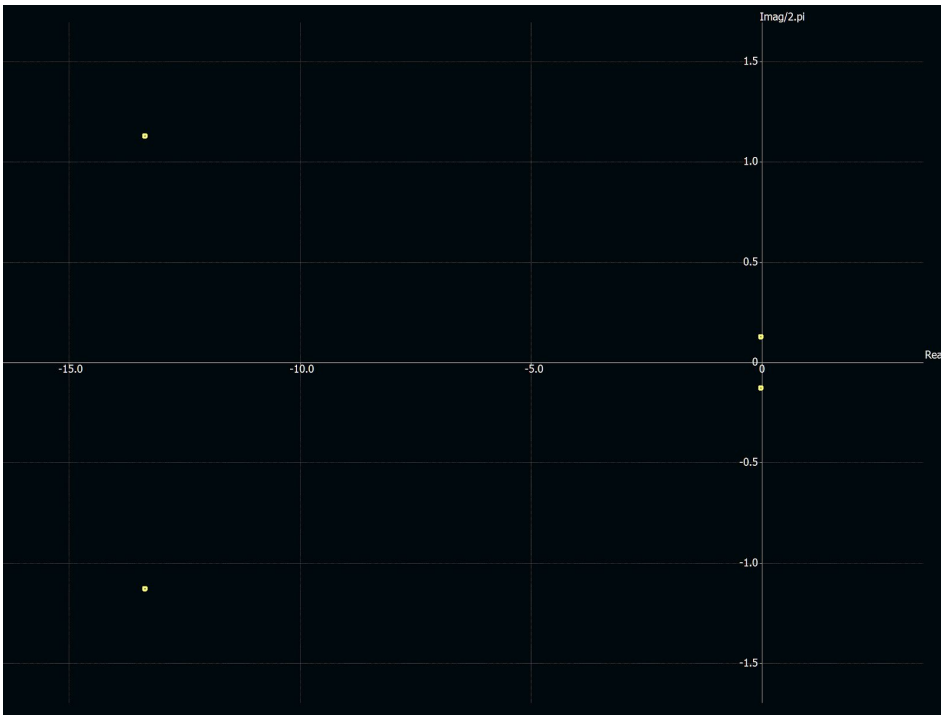

Figure 12: Longitudinal Root Locus Graph.

The size and location of the horizontal stabilizer was adjusted iteratively to achieve damped oscillations with small frequencies. The horizontal stabilizer is placed 4.50 inches below the main wing and 54 inches back from the leading edge of the main wing. Specific dimensions are listed in the table below as well as in the engineering drawing of the final design in the appendix.

	Span (in)	**Chord Length (in)**	**Area (ft^2)**
Horizontal Stabilizer+Elevator	53	14	5.15
Elevator	53	4	1.47

Table 4: Horizontal Stabilizer Dimensions

Lateral Stability

Lateral stability was also measured according to a root locus graph, shown in Figure 13 below.

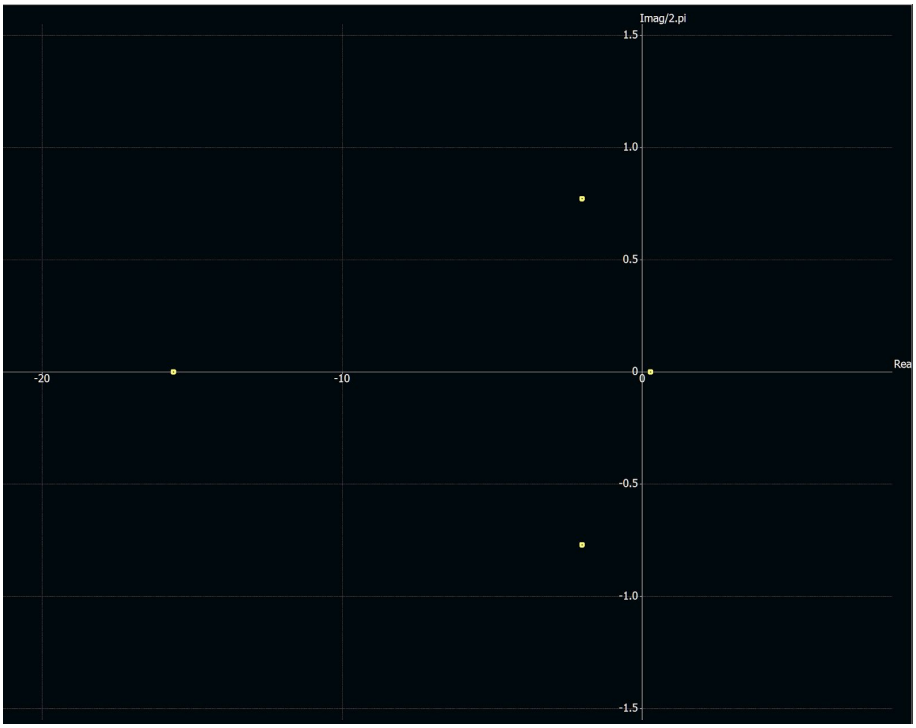

Figure 13: Lateral Root Locus Graph.

Again, points to the left of the imaginary axis reflect damped oscillations, and points further from the real axis indicate higher oscillatory frequencies. Lateral stability was achieved using a center of gravity positioned below the wing and a vertical stabilizer placed 4.50 inches below the wing and 46.5 inches back from the leading edge of the main wing. The final vertical stabilizer design is depicted in the following figure:

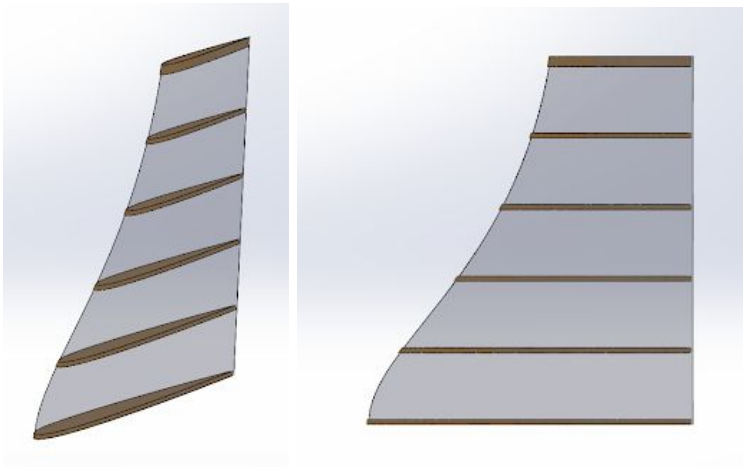

Figure 14: Skeleton of the vertical stabilizer with rudder.

There is still one point to the right of the imaginary axis in the root locus graph, however, indicating one mode of instability. This mode is characterized by a tendency to very slowly continue in the direction of a yaw/horizontal disturbance. The team found that the only way to correct this was to incorporate a large amount of dihedral on the main wing. This would severely complicate manufacturing, though. Since a small roll or yaw correction by the pilot would be sufficient to return the plane to normal flight, the team deemed the vertical stabilizer, low center of gravity, and piloting ability sufficient for lateral stability.

Lateral control is provided by the rudder and ailerons of the airplane. Recommended values for chord, span, and area ratios were used to size these control surfaces. The dimensions for the vertical stabilizer, rudder, and ailerons are listed in the two following tables as well as the engineering drawing found in the appendix.

	Height (in)	**Base Chord Length (in)**	**Top Chord Length (in)**	**Area (ft^2)**
Vertical Stabilizer+Rudder	18	16	7	1.40
Rudder	18	3	3	0.375

Table 5: Vertical Stabilizer Dimensions.

Chord Length (in)	**Span (in)**	**Area (ft^2)**
4	30	.833

Table 6: Aileron Sizing (for one aileron).

Propeller

Below in Figure 15 is a 3D graph that shows how the effective thrust changes with velocity. Each line represents a different propeller diameter with a calculated pitch that would give 1000 Watts for static thrust (when airspeed equals zero).

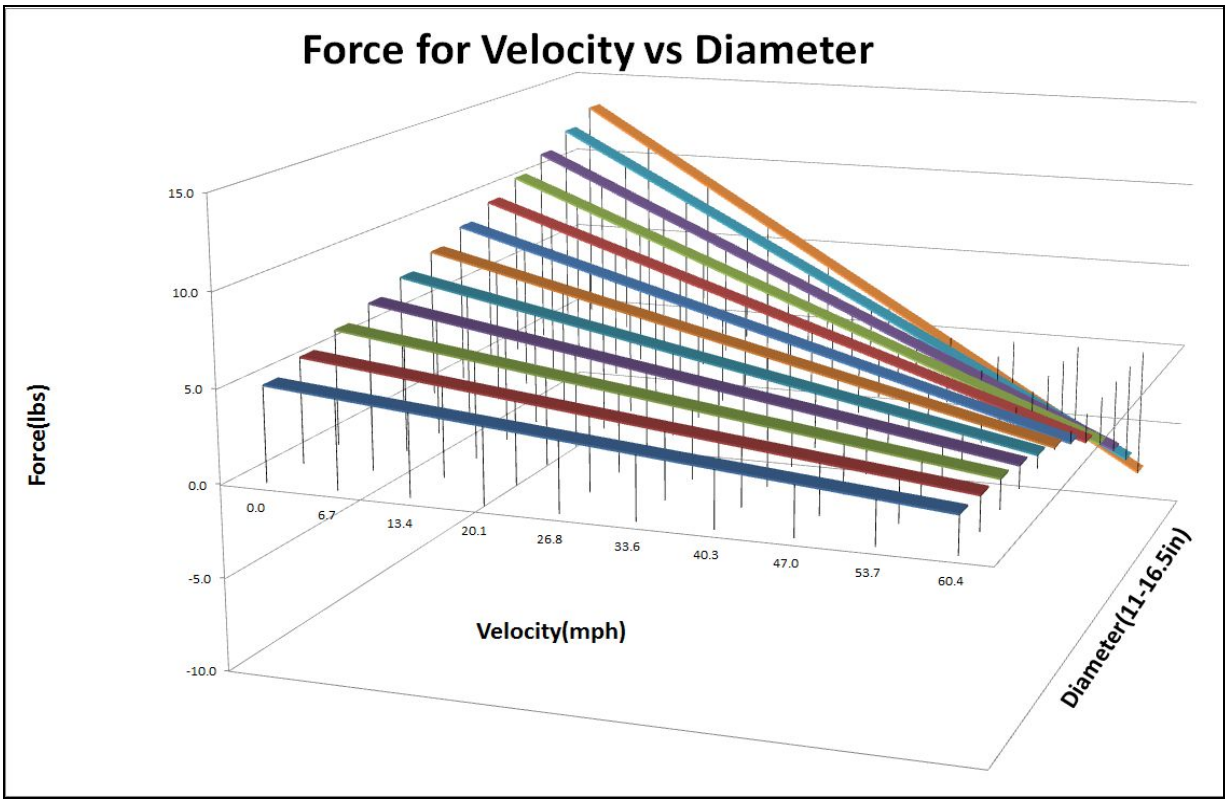

Figure 15: Force versus Velocity Graph for Different Diameter and Pitch Propellers.

This graph and the corresponding table values helps to identify the best theoretical propeller to pair with the airplane. (See appendix for the Dynamic Thrust Equation used to create this graph.)

From these calculations, the ideal combination is a 500 kV (or 500 rpm/V) motor and a 14-inch diameter propeller with a 7-inch pitch. This propeller combination is able to takeoff in the distance allowed and is able to carry the most weight while in flight.

Velocity (mph)	0.0	4.0	8.1	12.1	16.1	20.1	24.2	28.2	32.2	36.2
Thrust (lbs)	9.1	8.4	7.8	7.2	6.6	6.0	5.4	4.7	4.1	3.5
Power (Watts)	1064	843	781	720	658	597	535	473	412	350

Table 7: Ideal Motor and Propeller Theoretical Thrust.

The partial table above identifies the values for the ideal combination of motor and propeller corresponding to the 3D graph. This combination gives the highest thrust at the beginning, while also maintaining necessary thrust needed to equal the drag during flight.

Electronic Speed Controller (ESC)

The speed controller must be rated over or above the max possible amperes drawn. The maximum wattage is 1000 W and the voltage is 22.2 Volts so the maximum amperes is 45 Amps. Therefore the ESC must be over 45 Amps. The team chose a 70 Amps model based on availability of ESC's over 45 Amps.

HobbyKing Blueseries Brushless ESC: 70A

Maximum amperes used: $Amps = \frac{W}{V} = \frac{1000W}{22.2V}$ = **45 Amps**

Motor

The propeller above performs best when combined with a 500 kV motor. Using this motor with a 6 series (22.2V) battery, the maximum rpm of the motor is calculated to be about 10,000 rpm.

Turnigy Aerodrive SK3: 5045-500kV

Max Loading: 5-7S lipo | 58 Amps | 1350 W

Battery

The battery must be a 6 series battery (22.2 Volts) according to the rules. The battery must last at least 3 minutes of flight and able to provide enough amps for the max drawn by the motor. The battery used, listed below, is easily able achieve these conditions.

Turnigy Nano-tech 3000mAh, 6S, 25-50C

Capacity: 3000mAh; Voltage: 6S1P 22.2V; Discharge: 25C Constant; 50C Burst
Maximum current available from battery: $Amps = Capacity * C\ Rating = 3\ Amp\ hours * 25C$ = **75 Amps >** 45Amps maximum needed
Estimated wattage at maximum speed: = **350W** (see table 7)
Estimated flight time at maximum speed: $3\ Amp\ hours/(350W/22.2V) * 60\frac{min}{hour} \approx$ **11.3 minutes**

Wires and Connectors

The wires and connectors were chosen by keeping in mind the fact that they must be able to handle the maximum current of 45 Amps. The team chose a 12 awg (gauge) wire that can and will easily handle the maximum current rating. The plugs on the wires were all standardized XT60 connectors that are able to handle up to 60 Amps which exceeds the requirements outlined earlier.

Performance Analysis

The team developed a very thorough method for determining the weight capacity of an airplane for taking off within competition limits as well as carrying capacity during in-flight conditions. The approach centers around the C_D versus velocity graph obtained through CFD analysis in XFLR5.

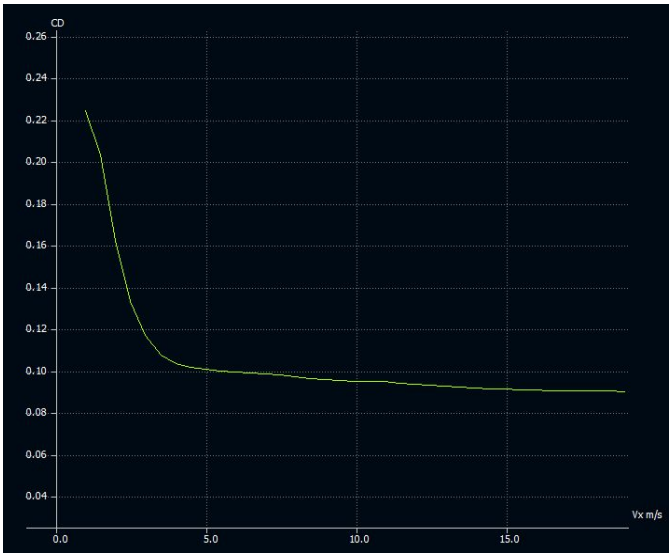

Figure 16: XFLR5 Graph of Drag Coefficient versus Velocity.

The graph above is generated by a list of data points obtained with the XFLR5 software. In order to make use of them in calculating thrust, the team wrote a program that created a piecewise continuous function based on those points. This function changes for each plane tested because each has different drag characteristics. Since the drag force is dependent on the drag coefficient, the following equation can then be used to calculate net thrust:

$$T_{net}(v) = T(v) - D(v) - f(v)$$

where $T_{net}(v)$ is the dynamic thrust generated by the propeller, D(v) is drag, and f (v) is friction between the airplane and runway. Acceleration at a specific velocity may then be calculated by simply dividing the net thrust by the mass of the aircraft. From the kinematic equations of constant acceleration,

$$X = x + vt + 0.5at^2$$

and

$$V(v) = v + at$$

the distance the plane travels in a very small time increment and its velocity after that time period can be calculated, as acceleration may be approximated as constant during small time periods. By performing those calculations in a loop until takeoff velocity is reached, the distance the plane travels while moving from rest to takeoff velocity is determined. Takeoff velocity is defined in this document as the velocity needed to achieve lift equal to the weight of the plane using the maximum lift coefficient. The value for takeoff distance was found to converge to two decimal places when the time increment reached 0.01 seconds. From this calculation, the team estimates that the plane can take off with a maximum gross weight of 43.65 lbs within the 200 ft runway limit.

However, while an airplane might be able to take off with a certain amount of weight it might not be able to maintain flight with that weight. To predict the maximum in-flight weight capacity of the plane, the velocity at which the propeller thrust and drag force are equal was calculated. For the 2017 aircraft this value was found to be approximately 38 mph. That velocity was then substituted into the following lift equation to find the maximum weight capacity in-flight:

$$L = \frac{1}{2}\rho v^2 A C_L$$

The result was 37.28 lbs. This is the limiting weight, as it is lower than the weight the plane could theoretically take off with. However, given the severe penalty for failing to carry all of the passengers the plane has seats for, the team did not design the airplane to fly with weight approaching the theoretical limit. The team allowed seats for 24 passengers at 0.125 lbs per passenger (tennis ball) and

0.50 lbs of luggage per passenger. With an estimated empty plane weight of 17 lbs the total weight of the plane including passengers and luggage will be 32 lbs, well below the theoretical capacity.

These calculations were done assuming the properties of air at sea level. As altitude increases the density of air varies, yielding different weight capacities at different heights. In accordance with the Technical Design Report and Technical Data Sheet requirements, the team captured the payload weight capacity vs altitude. To obtain this information the team calculated pressures and temperatures at various altitudes according to the following two equations:

$$p=p_0\left(1-\frac{Lh}{T_0}\right)^{\frac{gM}{RL}}$$

$$T=T_0-Lh$$

where p_0 is the pressure at sea level, L is the temperature lapse rate, h is the altitude, g is acceleration due to gravity, M is the molar mass of air, R is the universal ideal gas constant, and T_0 is the temperature at sea level. Air densities at altitudes ranging from sea level (0 ft) to 4000 ft were then be calculated according to the ideal gas law:

$$\rho=\frac{pM}{RT}$$

The limiting weight capacities of the final wing design at those heights were determined based on the corresponding air densities. The results are shown in a plot in the appendix.

Manufacturing

Manufacturing is expected to take approximately two weeks. The plane design has been optimized for ease of manufacturing and repair in case of crash. For example, the wing is easily detachable from the fuselage using only three bolts and the wing is backswept for ease of aileron construction. The structural ribs of the wing and stabilizers will be made of a lightweight balsa wood that will be cut into shape using 50 watt Epilog Fusion precision laser cutter. The laser cutter ensures a

very accurate airfoil shape, which is crucial for the plane to perform as predicted. The other wooden support structures, including fuselage, wing supports, and stabilizer supports will be made from pine wood, also cut per modeling using the laser cutter. The structures will be cut out with notches so that they will fit together easily. The wooden components will be glued together using cyanoacrylate glue and allowed to cure. Small hinges will be glued on at the control structures with space allotted for servo mounting. Finally, the stabilizers, fuselage, and wing will be covered with MonoKote and ironed to provide a smooth, aerodynamic finish.

Conclusions

The final design of the airplane was completed within the parameters set by the SAE Aero Design Challenge. The following chart summarizes the allowable and actual specifications of the design.

Specification	Allowable	Actual/Predictions
Takeoff Distance	200 ft	147 ft
Maximum Power	1000 W	1000 W
Battery Capacity	3,000 mAh	3,000 mAh
Battery Discharge Rate	25 C	25-50 C
Maximum Weight	55 lbs	32 lbs
Number of Passengers	NA	24
Center of Gravity, Empty (x_{CG}, y_{CG}) **Back from leading edge of the wing**	NA	(8.23”, 3.65”)

References

"Aircraft Weight and Balance Handbook." *AccessScience* (2007): n. pag. *FAA*. US Department of Transportation, 2007. Web. 25 Jan. 2016.

"SAE Collegiate Design Series." Results. SAE, n.d. Web. 18 Jan. 2016.

"Standard Pipe Schedules and Sizes Chart Table Data." *Standard Pipe Schedules and Sizes Chart Table Data*. Engineers Edge, LLC, 25 Jan. 2016. Web. 25 Jan. 2016.

Staples, Gabriel. "Propeller Static & Dynamic Thrust Calculation." *Electric RC Aircraft Guy*. 13 Apr. 2014. Web. 24 Jan. 2016.

UIUC Department of Aerospace Engineering. "UIUC Airfoil Data Site." UIUC Airfoil Data Site. UIUC Applied Aerodynamics Group, 1995-2012. Web. 10 Nov. 2012. <http://www.ae.illinois.edu/m-selig/ads/coord_database.html>.

Scott, Jeffrey A. "Ask Us - Aircraft Landing Gear Layouts." Aerospaceweb.org. N.p., 31 Oct. 2004. Web. 16 Jan. 2017.

List of Symbols and Acronyms

2D	Two dimensional	V(v)	Velocity
3D	Three dimensional	v	Initial velocity
A	Area	V	Max Velocity
a	Acceleration	W	Weight
C_D	Drag coefficient	X	Final distance
CFD	Computational Fluid Dynamics	x	Initial distance
C_L	Lift coefficient	μ	Dynamic viscosity
		ρ	Density
D	Drag	TU	University of Tulsa
ESC	Electronic Speed Controller		
f(v)	Friction between the airplane and runway	kV	rpm/Volt
L	Lift	rpm	Revolutions per Minute
NACA	National Advisory Committee for Aeronautics	mAh	milliamp hours
T(v)	Trust		
$T_{net}(v)$	Net Thrust		
t	Time		

Appendix

Payload Weight vs Altitude

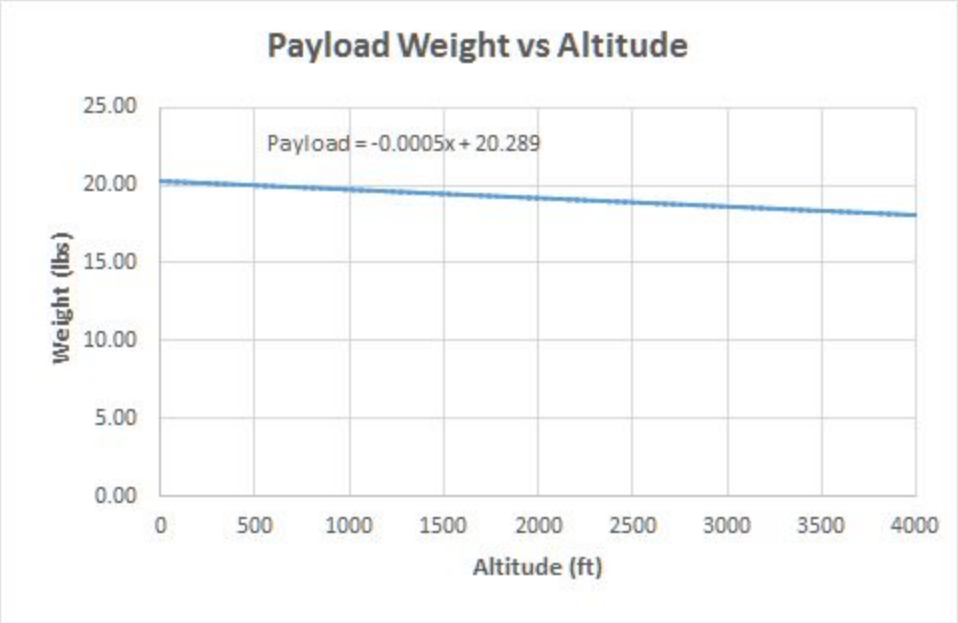

The process used to create this graph is discussed in the "Performance Analysis" section of this document.

Dynamic Thrust Calculations for Propeller Selection

F=thrust(lbs)

$$F = 4.3924x10^{-8} * RPM \frac{d^{3.5}}{\sqrt{pitch}} (4.23333x10^{-4} * RPM * pitch - V * 2.237) * .225$$

d= prop diameter. (in.)

rpm= propeller rotations/min.

pitch =propeller pitch (in.)

V= propeller forward velocity (mph)

(See Figure 16 and Table 7)

2D Drawing of the Plane

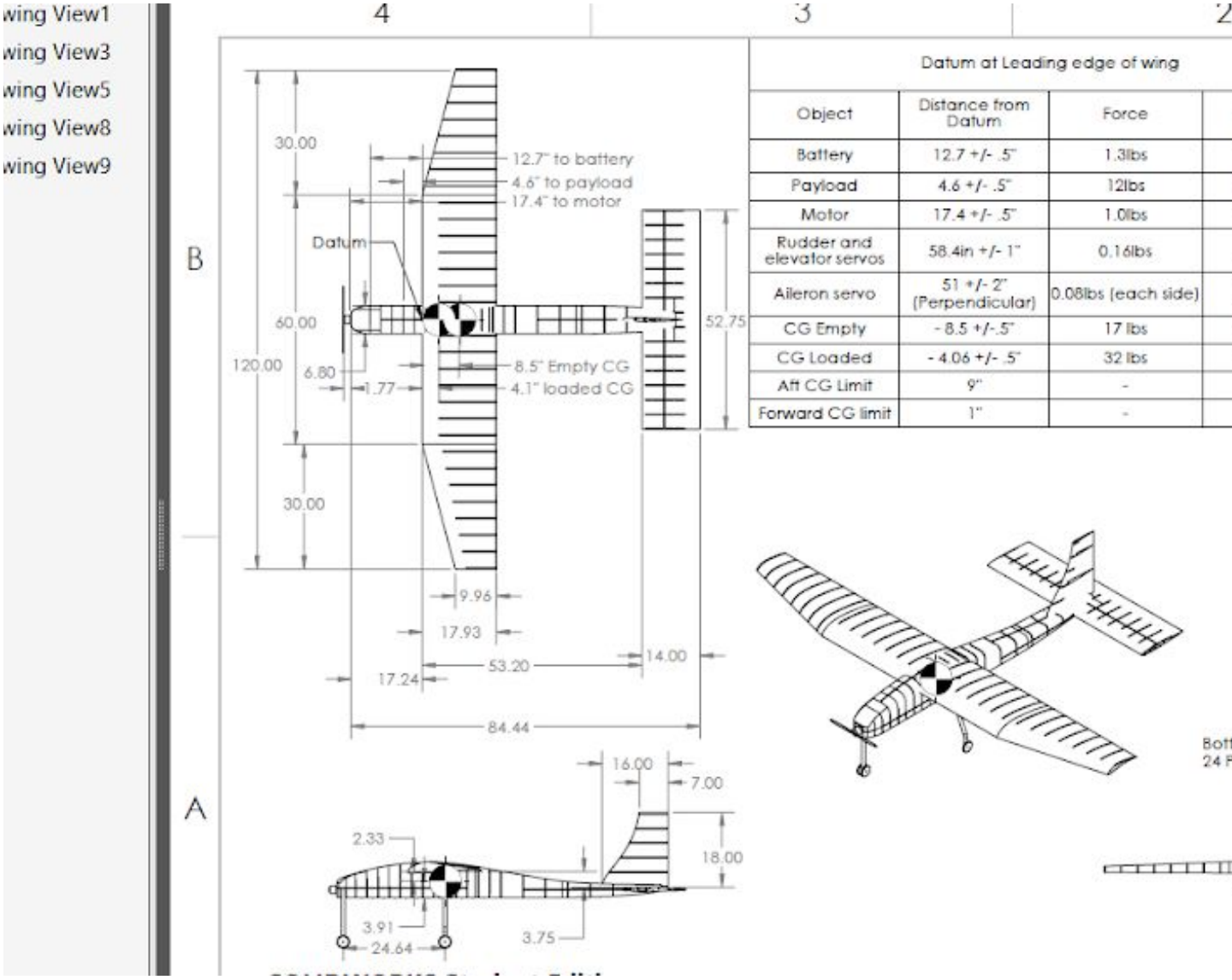

Datum at Leading edge of wing			
Object	Distance from Datum	Force	
Battery	12.7 +/- .5"	1.3lbs	
Payload	4.6 +/- .5"	12lbs	
Motor	17.4 +/- .5"	1.0lbs	
Rudder and elevator servos	58.4in +/- 1"	0.16lbs	
Aileron servo	51 +/- 2" (Perpendicular)	0.08lbs (each side)	
CG Empty	- 8.5 +/- .5"	17 lbs	
CG Loaded	- 4.06 +/- .5"	32 lbs	
Aft CG Limit	9"	-	
Forward CG limit	1"	-	